



Bayesian Bootstrap Filter Approach for GPS/INS integration

Khalid TOUIL¹, Abderrahim GHADI²

¹ FSTT-Abdelmalek Essaâdi University, Morocco, khalid.touil@gmail.com

² FSTT-Abdelmalek Essaâdi University, Morocco, ghadi05@gmail.com

Abstract

Inertial Navigation System (INS) and Global Positioning System (GPS) technologies have been widely used in a variety of positioning and navigation applications. Because the GPS and the INS complement each other, it is common practice to integrate the two systems. The advantages of GPS/INS integration is that the integrated solution can provide continuous navigation capability even during GPS outages. It is well known that Kalman filtering is an optimal real-time data fusion method for GPS/INS integration. However, it has some limitations in terms of stability, adaptability and observability. To solve this problem, we propose to use the Bayesian Bootstrap Filtering (BBF) for GPS/INS integration. Bootstrap filter is a filtering method based on Bayesian state estimation and Monte Carlo method, which has the great advantage of being able to handle any functional non-linearity and system and/or measurement noise of any distribution. Experimental result demonstrates that the bootstrap filter gives better positions estimate than the standard Extended Kalman filter (EKF).

Key words: GPS/INS integration, data fusion, Bayesian Bootstrap Filtering, Extended Kalman filter.

1. Introduction

The global positioning system (GPS) has been extensively used in navigation because of its accuracy and worldwide coverage [1, 2]. It is well established that GPS can provide accurate position, velocity and timing information under good satellite signal tracking environments. The limitations of GPS are related to the loss of accuracy in the

narrow-street environment, poor geometrical dilution on precision (GDOP) coefficient and the multipath reflections. So it is suitable to integrate the GPS with a different type of navigation system in order to reach a greater autonomy. From this point of view, the inertial navigation system (INS) is ideal [3, 4]. INS can provide continuous position, velocity, and also orientation estimates, which are accurate for a short term, but are subject to drift due to sensor drifts. The integration of GPS and INS can overcome the shortcomings of the individual systems, namely, the typically low rate of GPS measurements as well as the long term drift characteristics of INS. Integration can also exploit advantages of two systems, such as the uniform high accuracy trajectory information of GPS and the short term stability of INS. There have been a number of recent approaches to improving the performance of GPS/INS integration [5, 6, 7]. The Kalman filtering is an optimal real-time data fusion method for GPS/INS integration [8, 9], it has some limitations in terms of stability, adaptability and observability, etc. Different integration filters have also been investigated for example, the Extended Kalman Filter (EKF) [10, 11], the Quadratic Extended Kalman Filter (QEKF) [12], the Unscented Kalman Filter (UKF) [13]. The EKF is the traditional method for GPS/INS integration. Note that the accuracy of integrated navigation solution is directly related to the adequacy of the linearized error models. But for low quality inertial devices, the EKF may be unstable or even divergent [14] due to the large linearized errors. It is therefore highly desirable to have a solution that retains some of these nonlinearities. In this paper, we propose to use the Bayesian bootstrap filtering (BBF) [15, 16, 17] for GPS/INS integration.

The BBF is used in identification of hysteretic systems with slip [18], target tracking [19, 20] satellite attitude determination [21, 22, 23]. Bootstrap filter is a filtering method based on Bayesian state estimation and Monte Carlo method, which has the great advantage of being able to handle any functional non-linearity and system and/or measurement noise of any distribution. The BBF is independent on the initial state and can avoid the divergence problem, but its drawback is the heavy computational load in the update stage. The idea of this filtering method is to represent the required probability density function (PDF) as a set of random samples, rather than as a function over state space. As the number of samples becomes large, they can effectively provide an accurate representation of the required PDF. Estimations of states can then be obtained directly from the samples. The paper is organized as follows. Section 2 presents a mathematical model of integrated GPS/INS system. In the third section, a Bayesian bootstrap filtering algorithm is described. Experimental results are presented to demonstrate the accuracy of the proposed algorithm in section 4. Finally, conclusions are made in section 5.

2. Mathematical model of integrated GPS/INS system

In an INS, sensed accelerations and angular rates from an Inertial Measurement Unit (IMU) are transformed into position, velocity and attitude by solving a set of differential equations. GPS on the other hand delivers positions with relatively low accuracy but with a bounded error. INS and GPS have complementary properties and are therefore well suited for integration. There are different modes of integration [24, 25]. In this work, a tightly coupled GPS/INS system has been implemented [26]. This means primarily that GPS pseudo-ranges are used as inputs to the navigation filter rather than computed GPS positions.

2.1. State model

The state vector is composed of the INS error that is defined as the deviation between the actual dynamic quantities and the INS computed values: $\delta X = X - X_{INS}$. The state model describes the INS error dynamic behavior depending on the instrumentation and initialization errors. It is obtained by linearizing the ideal equations around the INS estimates as follow:

$$\delta X = f(X, U) - f(X_{INS}, U_{INS}) \quad (1)$$

$$\delta \dot{X} = \nabla f(X_{INS}, U_{INS}) \delta X \quad (2)$$

The state vector is usually augmented with systematic sensor errors:

$$\delta X = (\delta r, \delta \nu^n, \delta \rho, b_a, b_g, b, d) \quad (3)$$

where all the variables are expressed in the navigation frame NED (North, East, Down).

- $\delta r = (\delta \phi, \delta \lambda, \delta h)$ is the geodetic position error in latitude, longitude, altitude,
- $\delta \nu_N = (\delta \nu_E, \delta \nu_D)$ is the velocity error vector,
- $\delta \rho$ is the attitude (roll, pitch, yaw) error vector,
- b_a and b_g represent the accelerometers and gyroscopes biases,
- $b = c\tau_r$ and d are respectively the GPS clock offset and its drift. τ_r is the receiver clock offset from the GPS time and c is the speed of light $3 \times 10^8 m/s$.

For short-term applications, the accelerometers and gyroscopes can be properly defined as random walk constants $b_a = \omega_a$ and $b_g = \omega_g$. Note that the standard deviations of the white noises ω_a and ω_g are related to the sensor quality. The navigation solution also depends on the receiver clock parameters b and d models as $b = d + \omega_b$ and $d = \omega_d$, where ω_b and ω_d are mutually independent zero-mean Gaussian random variables [27]. For simplicity, denote as X (instead of δX) the state vector. The discrete-time state model takes the following form:

$$X_{INS,k+1} = A_k X_{INS,k} + \nu_k \quad (4)$$

where ν_k denote the dynamical zero-mean Gaussian noise vector with associated covariance matrix Σ_ν . The coupling effects between the components of $X_{INS,k}$ results in a block diagonal matrix A_k whose elements are detailed in many standard textbooks such as [27, chap. 6].

2.2 Measurement equation

The standard measurement of the GPS system is the pseudo-range. This defines the approximate range from the user GPS receiver antenna to a particular satellite. Consequently, the observation equation associated to the i^{th} satellite can be defined as:

$$\rho_i = \sqrt{(X_i - x)^2 + (Y_i - y)^2 + (Z_i - z)^2} + b + \omega_i \quad (5)$$

where, $i = 1, \dots, n_s$ (recall that n_s is the number of visible satellites).

The vectors $(x, y, z)^T$ and $(X_i, Y_i, Z_i)^T$ are respectively the positions of the vehicle and the i th satellite expressed in

the rectangular coordinate system WGS-84 [27, chap. 4]. In addition to the measurement of the pseudo-distance, we have also the measurement of delta-ranges. This latter characterizes the Doppler measurement (speed of distancing or approach of the visible satellites according to the respective axes under which they are seen since the receiver). For the i^{th} satellite, we model the observation of the delta-ranges by the following way:

$$\Delta\rho_i = R_i + b + \lambda_i \quad (6)$$

where,

$$R_i = \frac{(X_i - x)(\dot{X} - \dot{x}) + (Y_i - y)(\dot{Y} - \dot{y}) + (Z_i - z)(\dot{Z} - \dot{z})}{\sqrt{(X_i - x)^2 + (Y_i - y)^2 + (Z_i - z)^2}} \quad (7)$$

The vectors \dot{x} and \dot{y} are respectively the speeds of the vehicle and the i th satellite expressed in the rectangular coordinate system WGS-84. The position and the speed of the vehicle are transformed from the geodetic coordinate to the rectangular coordinate system as follows:

The vectors $(\dot{x}, \dot{y}, \dot{z})^T$ and $(\dot{X}_i, \dot{Y}_i, \dot{Z}_i)^T$ are respectively the speeds of the vehicle and the i th satellite expressed in the rectangular coordinate system WGS-84. The position and the speed of the vehicle are transformed from the geodetic coordinate to the rectangular coordinate system as follows:

$$\begin{cases} x = (N + h_{INS} + \delta h)\cos(\lambda_{INS} + \delta\lambda)\cos(\phi_{INS} + \delta\phi) \\ y = (N + h_{INS} + \delta h)\cos(\lambda_{INS} + \delta\lambda)\sin(\phi_{INS} + \delta\phi) \\ z = (N(1 - e^2) + h_{INS} + \delta h)\sin(\phi_{INS} + \delta\phi) \end{cases} \quad (8)$$

$$\begin{cases} \dot{x} = -(N + h_{INS} + \delta h)(\dot{\phi}_{INS} + \delta\dot{\phi})\sin(\phi_{INS} + \delta\phi)\cos(\lambda_{INS} + \delta\lambda) \\ \quad - (N + h_{INS} + \delta h)(\dot{\lambda}_{INS} + \delta\dot{\lambda})\cos(\phi_{INS} + \delta\phi)\sin(\lambda_{INS} + \delta\lambda) \\ \quad + (\dot{h}_{INS} + \delta\dot{h})\cos(\phi_{INS} + \delta\phi)\cos(\lambda_{INS} + \delta\lambda) \\ \dot{y} = -(N + h_{INS} + \delta h)(\dot{\phi}_{INS} + \delta\dot{\phi})\sin(\phi_{INS} + \delta\phi)\sin(\lambda_{INS} + \delta\lambda) \\ \quad + (N + h_{INS} + \delta h)(\dot{\lambda}_{INS} + \delta\dot{\lambda})\cos(\phi_{INS} + \delta\phi)\cos(\lambda_{INS} + \delta\lambda) \\ \quad + (\dot{h}_{INS} + \delta\dot{h})\cos(\phi_{INS} + \delta\phi)\sin(\lambda_{INS} + \delta\lambda) \\ \dot{z} = (N(1 - e^2) + h_{INS} + \delta h)(\dot{\phi}_{INS} + \delta\dot{\phi})\cos(\phi_{INS} + \delta\phi) \\ \quad + (\dot{h}_{INS} + \delta\dot{h})\sin(\phi_{INS} + \delta\phi) \end{cases} \quad (9)$$

where,

$$\begin{cases} \delta\nu_N = (N(1 - e^2) + h_{INS} + \delta h)\delta\dot{\phi} + \dot{\phi}_{INF}\delta h \\ \delta\nu_E = (N + h_{INS} + \delta h)\sin(\phi_{INS} + \delta\phi)\delta\dot{\lambda}_{INF} \\ \quad + (N + h_{INS})\cos(\phi_{INS} + \delta\phi)\delta\dot{\lambda} + \cos(\phi_{INS} + \delta\phi)\delta h\dot{\lambda}_{INS} \\ \delta\nu_D = -\delta\dot{h} \end{cases} \quad (10)$$

and $N = a/\sqrt{1 - e^2\sin^2\lambda}$. The parameters a and e denote the semi-major axis length and the eccentricity of the earths ellipsoid. These expressions (Eq. 8, Eq. 9 and Eq. 10) have to be substituted in (5) and (6) to obtain the highly nonlinear measurement equation:

$$Y_{GPS,k} = g(X_{INS,k}) + \beta_k \quad (11)$$

where $\beta_k = (\rho_1, \dots, \rho_n, \Delta\rho_1, \dots, \Delta\rho_n)$

is the pseudo-ranges and delta-ranges vector. In the Bayesian bootstrap filter, it is not necessary that the measurement noise β_k must be the white Gaussian. Now we can apply the bootstrap filter using the above state and measurement models.

3 Bayesian bootstrap filter

Bootstrap filter is relatively new concept in filtering. The advantage of bootstrap filter over Kalman and EKF is that the system does not have to be linear and the noise in the system can be non-Gaussian [15]. The Bayesian bootstrap filtering approach is to construct the conditional probability density function (PDF) of the state based on measurement information [15, 16, 17]. The conditional PDF can be regarded as the solution to the estimation problem. We shall briefly explain the recursive Bayesian estimation theory and the Bayesian Bootstrap filter.

3.1 Recursive Bayesian Estimation

The discrete-time stochastic dynamical system model can be described by the stochastic vector difference equation:

$$x_{k+1} = f(x_k, w_k)$$

where $f : \mathbb{R}^m \times \mathbb{R}^m \rightarrow \mathbb{R}^m$ is the system transition function and $w_k \in \mathbb{R}^m$ is a zero-mean noise process independent of the system states. The PDF of w_k is assumed to be known as $p_w(w_k)$. At discrete time, measurements are denoted by $y_k \in \mathbb{R}^m$, which are related to the state vector via the observation equation:

$$y_k = h(x_k, \nu_k) \quad (12)$$

where $h : \mathbb{R}^m \times \mathbb{R}^r \rightarrow \mathbb{R}^p$ is the measurement function, and $\nu_k \in \mathbb{R}^r$ is the observation noise, assumed to be another zero mean random sequence independent of both state variable x_k and the system noise w_k .

The PDF of ν_k is assumed to be known as $p_\nu(\nu_k)$. The set of measurements from initial time step to step k is expressed as $Y_k = \{y_i\}_{i=1}^k = 1$. The distribution of the initial condition x_0 is assumed to be given by $p(x_0/Y_0) = p(x_0)$.

The recursive Bayesian filter based on the Bayes rule can be organized into the time update state and the measurement update stage. The time update state can be constructed as:

$$p(x_k/Y_{k-1}) = \int p(x_k/x_{k-1}) \times p(x_{k-1}/Y_{k-1}) dx_{k-1} \quad (13)$$

where $p(x_k/Y_{k-1})$ is determined by $f(x_{k-1}, w_{k-1})$ and the known PDF $p_w(w_{k-1})$. Then at time step k , a measurement y_k becomes available and may be used to update the prior according to the Bayes'rule:

$$p(x_k/Y_k) = \frac{p(y_k/x_k) \times p(x_k/Y_{k-1})}{\int p(y_k/x_k) \times p(x_k/Y_{k-1})} \quad (14)$$

where the conditional PDF $p(y_k/x_k)$ is determined from the measurement model and the known PDF, $p_\nu(\nu_k)$. The

embodiment of the recursive Bayesian filter is very hard and laborious work because closed form solutions of the equations (14) and (15) do not exist, or are difficult to find, therefore should be implemented numerically with high computational load.

3.2 Bayesian Bootstrap filter

From the recursive Bayesian filter the BBF algorithm can be described as follow. The BBF is an algorithm for propagating and updating the random samples from the pdf of the state. Therefore, the BBF may be considered as an approximation to be the recursive Bayesian filter. Suppose we have a set of random samples $x_{k-1}(i) : i = 1, \dots, N$ PDF $p(x - k - 1/Y_{k-1})$. Here, N is the number of bootstrap samples.

The filter procedure is as follows:

1. Prediction: Each sample from PDF $p(x_{k-1}/Y_{k-1})$ is passed through the system model to obtain samples from the prior at time step k :

$$x_k(i) = f(x_{k-1}(i), w_k(i)), \tag{15}$$

where $w_k(i)$ is a sample draw from PDF of the system noise $p_w(w_k)$.

2. Update: On receipt of the measurement y_k , evaluate the likelihood of each prior sample and obtain the normalized weight for each sample:

$$q_i = \frac{p(y_k/x_k^*(i))}{\sum_{j=1}^N p(y_k/x_k^*(j))} \tag{16}$$

This define a discrete distribution over $x_k(i) : i = 1 \dots, N$, with probability mass q_i associated with element i . Now resample N times from the discrete distribution to generate samples $\{x_k(i) : i = 1, \dots, N\}$, so that for any j , $Prob_{x_k}(j) = x_k(i) = q_i$. The above steps of prediction and update form a single iteration of the recursive algorithm. To initiate the algorithm, N samples $x_1(i)$ are drawn from the known initial PDF $p(x_1/Y_0) = p(x_1)$. These samples feed directly into the update stage of the filter. We contend that the samples $x_k(i)$ are approximately distributed as the required PDF $p(x_k/Y_k)$. Repeat this procedure until the desired number of time samples has been processed. The basic algorithm is very simple and easy to program. The re-sampling update stage is performed by drawing a random sample u_i from the uniform distribution over $(0, 1]$. The value $x_k^*(M)$ corresponding to:

$$\sum_{j=0}^{M-1} q_j < u_i \leq \sum_{j=0}^M q_j \tag{17}$$

where $q_0 = 0$, is selected as a sample for the posterior. This procedure is repeated for $i = 1, \dots, N$. It would also be straightforward to implement this algorithm on

massively parallel computers, raising the possibility of real time operation with very large sample sets. The number N depends on the dimension of the state space, the typical overlap between the prior and the likelihood $p(y_k/x_k)$ and the required number of time steps [15].

4 Simulation results

The analysis of some simulations will enable us to evaluate the performance of the utilization of the BBF. Here, we present two examples which illustrate the operation of the bootstrap filter. Estimation performance is compared with the standard EKF. The first example is an univariate nonstationary growth model taken from references [28, 29]. The second is a navigation problem using GPS and INS systems.

4.1 Example1

Consider the following nonlinear model [28]:

$$x_k = 0.5x_{k-1} + 25x_{k-1}/(1 + x_{k-1}^2) + 8\cos(1.2(k - 1)) + w_k \tag{18}$$

$$y_k = x_k^2/20 + \nu_k \tag{19}$$

where w_k and ν_k are zero-mean Gaussian white noise with variances 10 and 1 respectively. This example is severely nonlinear, both in the system and the measurement equation. Note that the form of the likelihood $p(y_k/x_k)$ adds an interesting twist to the problem. For measurement $y_k < 0$ the likelihood is unimodal at zero and symmetric about zero. However, for positive measurements the likelihood is symmetric about zero with modes at $\pm (20y_k)^{1/2}$. The initial state was taken to be $x_0 = 0.1$ and Fig. 1 shows a 50 step realization of Eq. 19. The EKF and bootstrap filters were both initialized with the prior PDF $p(x_0) = N(0, 2)$. Fig. 2 shows the result of applying the EKF to 50 measurements generated according to Eq. 20. The true state is represented by a solid line, EKF mean is given as a dashed lines. Fig. 3 shows the result of directly applying the bootstrap algorithm of section 3.2 with a sample size of $N = 500$. The dashed line gives the bootstrap estimate of posterior mean. Fig. 4 shows, the posterior can be bimodal in this example. At a couple of time steps, the actual state is just outside these percentile estimates, and quite often it is close to one of the limits. However, most of the time the actual state is very close to the posterior mean and performance is obviously greatly superior to the EKF. Running the bootstrap filter with larger sample sets gave results indistinguishable from Fig. 3, and this is taken as confirmation that our sample set size is sufficient. The relatively high system noise probably accounts for the reasonable performance of the basic algorithm using only 500 samples: the system noise

automatically roughens the prior samples. Fig. 4 shows estimates of the posterior density from both the bootstrap filter and the EKF at $k = 34$. The bootstrap PDF is a kernel density estimate [30] reconstructed from the posterior samples. It has a bimodal structure, with the true value of x_{34} located close to be larger mode. The Gaussian PDF from the EKF is remote from the true state value at this time step.

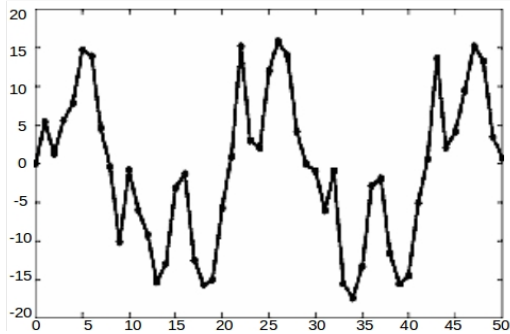


Fig. 1. 50 point realization of Eq. 19.

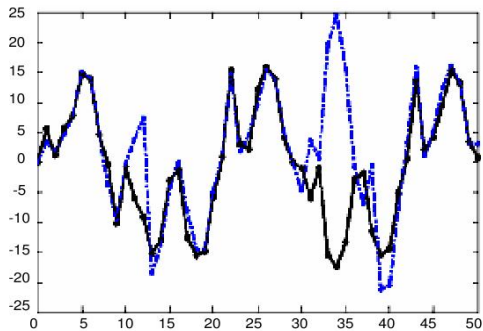


Fig. 2. EKF estimate of posterior mean.

4.2 Example 2

The kinematics data used were generated by SatNav Toolbox for Matlab created by GPSof. A GPS-INS simulation can be divided into three parts:

- Trajectory: the vehicle dynamics is simulated according to position-velocity- acceleration model.
- INS data: the INS estimates of the vehicle dynamics are then computed for inertial sensors with an accelerometer bias of $750g$ and a gyroscope bias of $3deg/h$.
- GPS data: the pseudo-ranges and delta-ranges corresponding to the visible satellites from the vehicle are

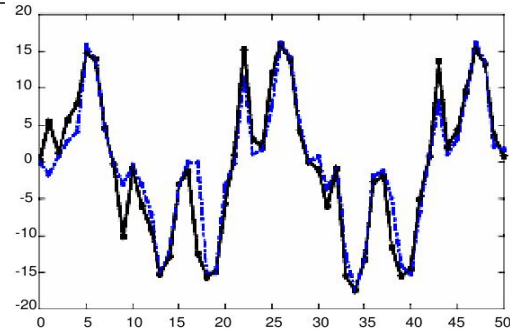


Fig. 3. Bootstrap filter estimate of posterior mean.

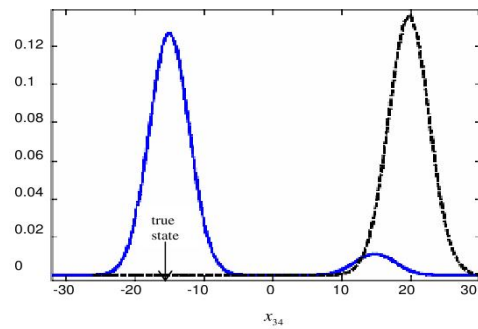


Fig. 4. Estimated posterior PDF at time step 34.

evaluated (the standard deviations of the GPS measurements noises are chosen as $\sigma = 10$ for pseudo-range and $\sigma_\lambda = 5$ for delta-range).

The performance of the BBF is studied for the estimation of latitude-drift, longitude-drift, altitude-drift and velocities-drifts. It should be noted that the number of particles is fixed at 2000. The figures (Fig. 5 to Fig. 9) represent respectively the actual (solid line) and estimations (dashed line) of latitude-drift (meter), longitude-drift (meter), altitude drift (meter), north-velocity-drift (meter/second) and down-velocity-drift (meter/second) according to temps (second). Note that the INS drifts reach about a couple of kilometers for simulation duration of 1200 seconds. These figures show the good tracking performance of the BBF: average error between the actual and estimated drops below 3 meter in position and 2 meter/second in velocity.

The results obtained with the EKF and the BBF are compared for simulation duration of 12000 second. For each method, the horizontal positioning root mean square error and the horizontal velocity root mean square error are com-

peted from 100 Monte Carlo runs. Fig. 10 and Fig. 11 shows the results obtained with the EKF (solid line) and BBF (dashed line). In Fig. 10, we note that the both filters have the same precision. It is due to the dynamics errors which are reasonable (where the local linearization is possible). However, in Fig. 11 the precision of the BBF is relatively better than the EKF. It should be noted that on the 100 Monte Carlo runs, the EKF diverged five times whereas the BBF diverged just once. Finally a complete GPS signal outage of 50 seconds was introduced within the GPS data and both filters were used to predict the INS dynamic, during this period. We simulated GPS outages over time intervals: $T_1 = [50, 60]$, $T_2 = [150, 160]$, $T_3 = [200, 210]$, $T_4 = [300, 310]$ and $T_5 = [350, 360]$. The root mean square errors of the two methods in this period are compared in Tab. 1. Time is computation time using Matlab in our implementation. The BBF needs more computing time than the EKF.

5 CONCLUSIONS

This paper studied a Bayesian Bootstrap Filter (BBF) algorithm to GPS/INS integration system. This filter has show interesting results for the proposed application. A comparison with other estimation strategies (such as the EKF) is currently under investigation. In the simulation results, we showed that the BBF can be an alternative solution to the classical EKF to solve the nonlinear GPS/INS. It was also shown that in the presence of GPS outage the BBF gives the better results than the EKF. The results show that integrated system can contribute to high-precision positioning in terms of performance. A comparison in critical situations with real data (such as loss of observability or presence of multipath) is currently under investigation in the future researches.

References [1] A. Leick, GPS satellite surveying, John Wiley, 1995.

[2] B. W. Parkinson, J. J. Spilker et al, Global Positioning System: Theory an Applications, Vols. I & II, AIAA, Inc., New York, 1996.

[3] K. R. Britting, Inertial Navigation System Analysis, John Wiley & Sons, Inc., 1971.

[4] M. S. Grewal, L. R. Weil and A. P. Andrews, Global Positioning Systems, Inertial Navigation, and Integration, John Wiley & Sons, Inc., 2001.

[5] R. Wolf, B. Eissfeller, and G. W. Hein, A Kalman filter for the integration of a low cost INS and attitude GPS, Proceedings on International Symposium on Kinematic Systems in Geodesy, Geomatics and Navigation, pp. 143-150, 1997.

[6] K. W. Chiang and N. El-Sheimy, INS/GPS Integration Using Neural Networks for Land Vehicle Navigation

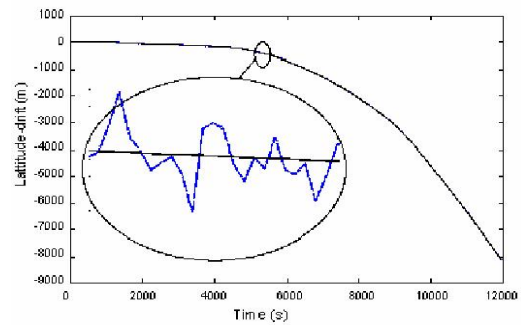


Fig. 5. Estimation of the latitude-drift (meter).

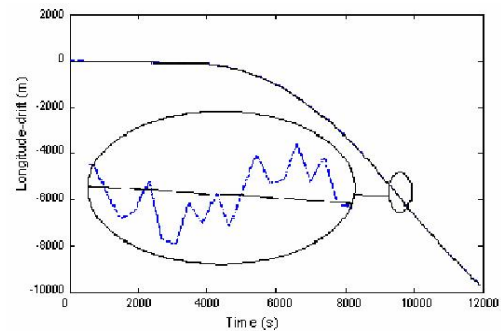


Fig. 6. Estimation of the longitude-drift (meter).

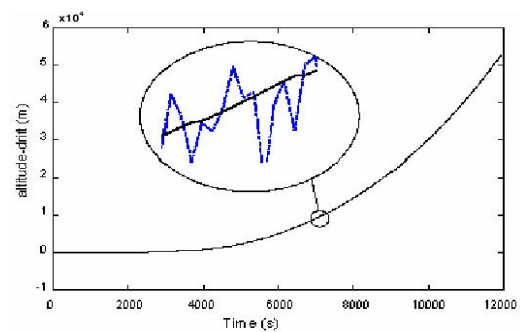


Fig. 7. Estimation of the altitude-drift (meter).

Tab. 1. Root mean square errors during satellites outage.

	Horizontal positioning	Horizontal velocity
EKF	23.4 meter	12.73 meter/sec
BBF	5.9 meter	3.65 meter/s

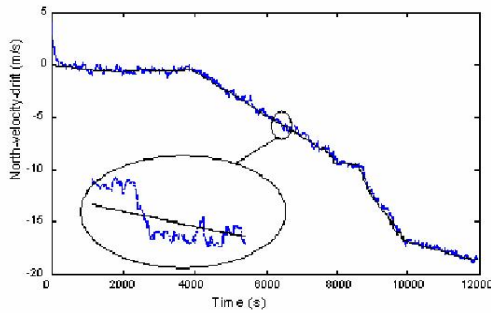


Fig. 8. Estimation of north-velocity-drift (meter/second).

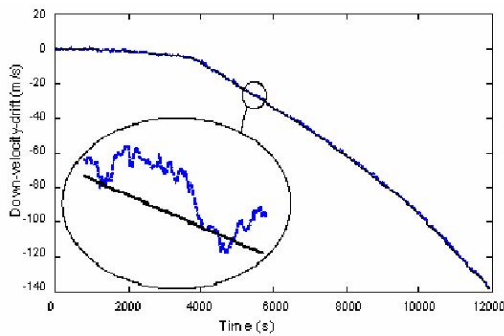


Fig. 9. Estimation of down-velocity-drift (meter/second).

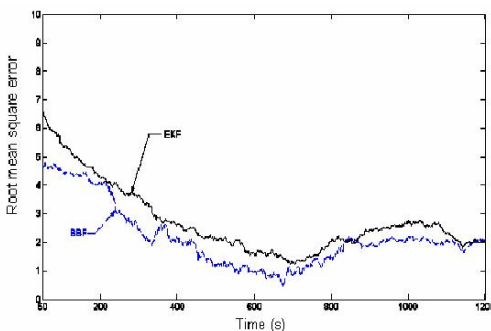


Fig. 10. Horizontal positioning root mean square error for EKF and BBF.

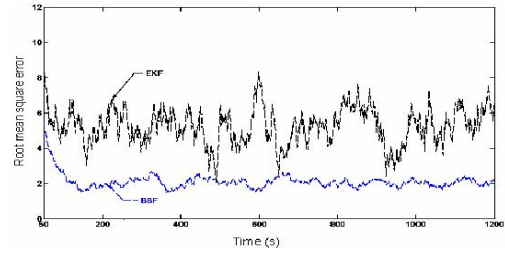


Fig. 11. Horizontal velocity root mean square error for EKF and BBF.

Applications, Proceedings of the ION GPS, pp. 535-544, 2002.

[7] E. H. Shin, A Quaternion-Based Unscented Kalman Filter for the Integration of GPS and MEMS INS, Proceedings of the ION GNSS, pp. 1060-1068, 2004.

[8] A. H. Mohamed and K. P. Schwarz, Adaptive Kalman filtering for INS/GPS, Journal of Geodesy, pp. 193-203, 1999.

[9] C. Hide, F. Michaud and M. Smith, Adaptive Kalman filtering algorithms for integrating GPS and low cost INS, IEEE Position Location and Navigation Symposium, Monterey California, pp. 227-233, 2004.

[10] J. Frang, G. Shen and D. Wan, Establishment of an Adaptive Extended Kalman Filter Model for a GPS/DR Integrated Navigation System for Urban Vehicle, Control Theory and Applications, Vol. 15, No. 3, pp. 385-390, 1998.

[11] F. A. Faruqi, K. J. Turner, Extended Kalman filter synthesis for integrated global positioning/inertial navigation systems, Applied Mathematics and Computation, 115, (2- 3), pp. 213-227, 2000.

[12] W. Wang, Z. Y. Liu and R. R. Xie, Quadratic extend Kalman filter approach for GPS/INS integration, Aerospace Science and Technology 10, pp. 709-713, 2006.

[13] R. Van der Merwe, , Wan E. A. and S. Julier, Sigma-Point Kalman Filters for Nonlinear Estimation and Sensor-Fusion: Applications to Integrated Navigation, In Proceedings of the AIAA Guidance, Navigation & Control Conference (GNC), Providence, Rhode Island, August, 2004.

[14] M. S. Grewal and A. P. Andrews, Kalman Filtering: Theory and Practice, Prentice-Hall, New Jersey, 1993.

[15] N.J. Gordon, D.J. Salmond, A.F.M. Smith, Novel approach to nonlinear/non-Gaussian Bayesian state estimation, IEE Proc.-F, 140, pp. 107-113, 1993.

[16] S. Cho and J. Chun, Bayesian Bootstrap Filtering for the Satellite Attitude Determination Using a Star Sensor, Proceedings of SPIE Vol. 4477, pp. 88-95, 2000.

[17] S. J. Li, Y. Suzuki, M. Noori, Improvement of parameter estimation for non-linear hysteretic systems with

slip by a fast Bayesian bootstrap filter, International Journal of Non-Linear Mechanics, 39, pp. 1435-1445, 2004.

[18] S. J. Li, Y. Suzuki, M. Noori, Identification of hysteretic systems with slip using bootstrap filter, Mechanical Systems and Signal Processing, 18, pp. 781-795, 2004.

[19] N. Gordon, A hybrid bootstrap filter for target tracking in clutter, Proceeding of the American Control Conference, pp. 628-632, 1995.

[20] H. M. Sun and Y. T. Lin, A Mixture Bootstrap Filter for Maneuvering Target Tracking, Proceedings of 2006 CACS Automatic Control Conference, pp. 494-499, 2006.

[21] S. Kim and J. Chun, Satellite Orbit Determination Using a Magnetometer-Based Bootstrap Filter, Proceedings of the American Control Conference, pp. 792-793, 2000.

[22] S. Cho and J. Chun, Satellite Attitude Acquisition Using Dual Star Sensors with a Bootstrap Filter, Proceedings of IEEE, Vol. 2, pp. 1723-1727, 2002.

[23] F. Jian-Cheng and N. Xiaolin, Autonomous celestial orbit determination using Bayesian bootstrap filtering and EKF, Proc. SPIE, Vol. 5253, pp. 216-222, 2003.

[24] A. Hiliuta, R. Jr. Landry and F. Gagnon, Fuzzy correction in a GPS/INS hybrid navigation system, IEEE Trans. Aerospace and Electronic Systems, Vol. 40, No. 2, pp. 591-600, April 2004.

[25] X. He, Y. Chen and H. B. Iz, A reduced-order model for integrated GPS/INS, IEEE AES Systems Magazine, pp. 40-45, MARCH 1998.

[26] W. L. Ling, H. K. Lee and C. Rizos, GPS/INS Integration: A performance sensitivity analysis, Wuhan University Journal of Natural Sciences, Vol. 8, No. 2B, 508-516, 2003.

[27] M. R. Robert, Applied Mathematics in Integrated Navigation Systems, AIAA Education Series, 3rd Edition, 2007.

[28] G. Kitagawa, Non-Gaussian state-space modeling of non-stationary time series (with discussion), J. Amer. Statistical Assoc., 82, pp. 1032-1063, 1987.

[29] B. P. Carli, N. G. Polson and D. S. Stoffer, A Monte-carlo approach to nonnormal and nonlinear state space modeling, J. Amer. Statistical Assoc., 87, pp. 493-500, 1992.

[30] B. W. Silverman, Density estimation for statistics and data analysis, Chapman & Hall, London, 1986.